

Extracting and Mathematical Identifying Form of Stationary Noise in X-ray Images

Akihiro Sugiura^{1,2*}, Kiyoko Yokoyama¹, Hiroki Takada³, Akiko Ihori², Naruomi Yasuda² and Takahiro Yoshida²

¹Graduate School of Design and Architecture, Nagoya City University, 2-1-10 Kitachikusa, Chikusa-ku, Nagoya 464-0083, Japan

²Department of Radiological Technology, Gifu University of Medical Science, 795-1 Nagamine Ichihiraga, Seki, Gifu 501-3892, Japan

³Graduate School of Engineering, University of Fukui, 3-9-1 Bunkyo, Fukui, Fukui 910-8507, Japan

*E-mail address: asugiura@u-gifu-ms.ac.jp

(Received November 14, 2010; Accepted April 9, 2011)

Image noise may prevent proper diagnostic X-ray imaging. This study is aimed at developing new noise rejection methods using a mathematical model that describes the form of X-ray image noise. Stationary noise is one type of noise found in X-ray images. Stationary noise is nonstochastic and appears independent of the radiographic factors. In this paper, we verify methods for identifying stationary noise using a polynomial regression model, and extracting such noise from X-ray images obtained from a CR system. The results of this study demonstrate that stationary noise can be extracted with high precision using a particular low-pass filter frequency. We found that a regression model for greater than second-degree polynomials can be applied for roughly identifying stationary noise. However, the fitting accuracy of the regression curve is not significantly improved in terms of the amount of multiplication required when increasing the degree of the polynomial regression model.

Key words: X-ray Image, Nonstochastic Noise, Stationary Noise, Polynomial Regression Model and CR System

1. Introduction

With the advancing digitization of radiographic imaging systems, digital X-ray imaging systems are being used in many medical facilities. Digital X-ray images obtained from these systems are widely used in many clinical fields such as diagnoses and mass-screening, as they do not require a processing procedure, can easily be subjected to image processing, and can easily be compared with images from prior examinations. Among digital X-ray images, those obtained from CR (computed radiography) or FPD (flat panel detector) systems are some of the most basic images used in determining the condition of a patient (Kono and Adachi, 2008). To improve the accuracy of diagnostic imaging, it is important to be able to vividly extract only information on a subject. This is achieved by removing from the images any existing noise that may prevent the detection of important clues, such as the source of the patient's condition.

A selective multi-frequency process has been generically performed for noise reduction in digital X-ray imaging systems (Yamada and Murase, 2005). This noise-reduction process is based on the characteristics of the images, including those of the subject. However, because both noise components and diagnostically important signals uniformly undergo the noise-reduction process, it is highly possible that this process does not selectively and completely remove only the noise contents. To solve this problem, we have therefore attempted to improve the diagnostic accuracy by developing a noise-rejection method that accurately realizes

the noise-generating mechanism related to the X-ray imaging system mathematically (in this paper, the authors define an X-ray imaging system to include an X-ray generator). Unlike a noise-reduction method using a conventional X-ray imaging process, the objective of this study is to develop a noise-rejection method using a mathematical model that realizes an accurate digital X-ray imaging system; the mathematical model may also realize the noise-generating mechanism. In diagnostic imaging, medical judgment of normality or abnormality is performed based on information of the signal forms found in diagnostic images: the term “signal form” indicates a particular signal's figure or pattern. Image noise may cause an inter-reader to make an improper medical judgment, because such noise may distort information of the signal form. Hence, mathematically identifying, and further modeling, the form of an image noise may contribute toward improving the accuracy of diagnostic imaging.

In identifying a suitable mathematical model, we have to consider the characteristics of the noise components of the X-ray imaging systems as such characteristics consist of various factors (Rossmann, 1963; Barnes, 1982; Ogawa *et al.*, 1995). Noise superimposed onto an X-ray image consists of both stochastic and nonstochastic noise (Dobbins *et al.*, 2006). One type of stochastic noise is quantum noise caused by a fluctuation of radiated photons. Another type is electrical noise attributed to the X-ray imaging system. On the other hand, non-stochastic noise includes fixation noise attributed to the X-ray imaging system. These noise components are always superimposed onto X-ray images. The aim of this study is to perform the mathematical iden-

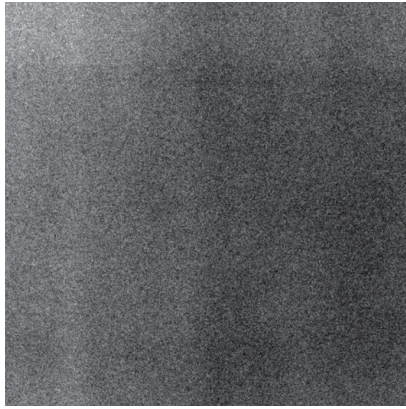


Fig. 1. X-ray images with 2 mAs (these images share the same window widths to integrate the noise hue).

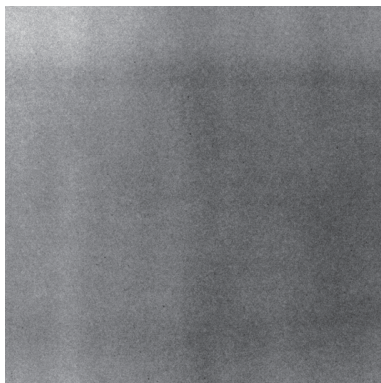


Fig. 2. X-ray images with 20 mAs (these images share the same window widths to integrate the noise hue).

tification of non-stochastic low-frequency noise (stationary noise) superimposed onto X-ray images from a CR system. We then aim to develop a noise rejection method using a mathematical model that realizes an accurate digital X-ray imaging system.

2. Stationary Noise

Stationary noise is a noise component that appears independent of the radiographic factors in the X-ray images. Figures 1 and 2 show digital X-ray images without a subject that were taken from the same CR system with different radiographic factors. The radiographic factors in Fig. 1 are 70 kV and 2 mAs (a low-dose setting), while those in Fig. 2 are 70 kV and 20 mAs (a high-dose setting). Compared with Fig. 1, Fig. 2 shows a decrease in spike-like noise caused by fluctuations in the radiated photons. However, we can find a comprehensive variation of density (pixel value) at the same position in each image. This fluctuation component is stationary noise. In stationary noise, there is a nonuniform distribution of X-ray emissions attributed to the architecture of the X-ray target, structural nonuniformity of the X-ray acceptance surface (structural nonuniformity of the imaging plate (IP)), nonuniformity in the sensitivity of the IP read-out systems, and so on.

A frequency analysis is generally used for the evaluation of noise in X-ray images. Dobbins *et al.* (2006) stated that

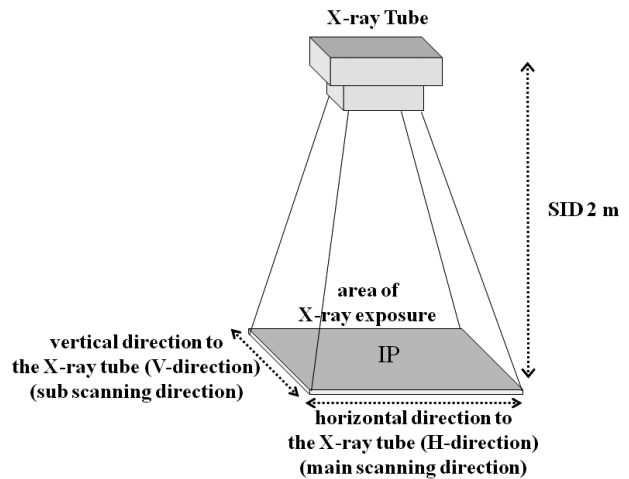


Fig. 3. Geometric arrangement of the X-ray exposure.

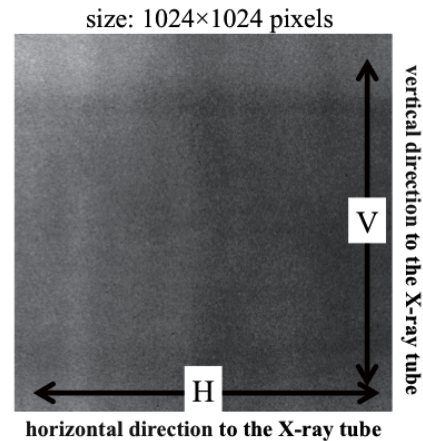


Fig. 4. Direction of each line profile in the X-ray images.

when performing a frequency analysis, an evaluation of the noise characteristics should be based on X-ray images that have been cleared of stationary noise. On the other hand, because stationary noise interferes considerably with diagnostic imaging, Kunitomo *et al.* (2010) stated that an evaluation of noise characteristics should be based on X-ray images that include this type of noise component; however, the direct current component should be removed to prevent leakage-based errors. We also believe that this type of noise component prevents accurate diagnostic imaging. Therefore, stationary noise should be removed completely using our suggested method.

2.1 Examination of stationary noise extraction method

In the mathematical identification of stationary noise, the problem is how to extract stationary noise X-ray images that include various noise components. Therefore, to solve this problem, we consider the characteristics of stationary noise and accordingly suppose that each image obtained from the same X-ray imaging system with different radiographic factors and processed by a low-pass filter (LPF) of a specific frequency shares the same distribution profile. Based on this supposition, we verified whether this presumption was correct by using the X-ray images obtained from the same

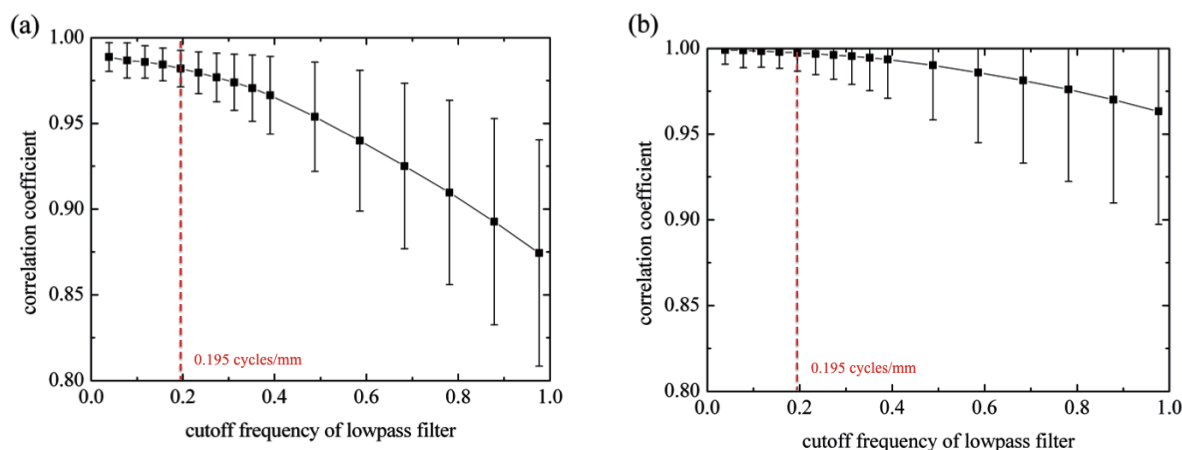


Fig. 5. Changes in the correlation coefficient based on changes in the cutoff frequency: (a) direction vertical to the X-ray tube (V-direction), and (b) direction horizontal to the X-ray tube (H-direction).

X-ray imaging system at different X-ray doses and with a gradual change in the LPF.

2.1.1 Subjects and methods To obtain digital X-ray images without a subject, we performed a uniform X-ray exposure using an X-ray generator (Shimazu Co., Ltd.) and IP (Fuji Film Co., Ltd.). The geometric disposition of the X-ray exposure had a source-interface distance (SID) of 2 m. The exposure area was reduced to the size of the IP, as shown in Fig. 3. For the radiographic factors, we set the tube voltage to 70 kV, and the dose settings to 2 (low setting) and 20 mAs (high setting). Altogether, the X-ray doses of these images differed by around a factor of 10. Next, the X-ray images were created using an A/D conversion in a CR system (Fuji Film Co., Ltd.). Finally, we acquired the images (matrix size, 2510×2000 ; pixel pitch, 0.1 mm; Nyquist frequency, 5 cycles/mm) from the CR system. Next, to extract the stationary noise, the images obtained from the CR system were processed using an LPF (cutoff frequency, 0.03 to 1 cycles/mm) processed through Image J imaging software. Then, to verify the consistency of both images, 1,024 line profiles ($n = 1,024$) with constricted pixel values in the vertical (V-direction) and horizontal (H-direction) directions to the X-ray tube were extracted as analysis objects from the center of the X-ray images after processing through an LPF with different cutoff frequencies.

To evaluate the consistency of each line profile, when the line profiles of the 2 mA and 20 mA images were set as $\{x_i | i = 1, 2, 3, \dots, 1024\}$ and $\{y_i | i = 1, 2, 3, \dots, 1024\}$, respectively, we calculated their correlation coefficients using Eq. (1):

$$r = \frac{\sum(x_i - \bar{x})(y_i - \bar{y})}{\sqrt{\sum(x_i - \bar{x})^2} \sqrt{\sum(y_i - \bar{y})^2}}. \quad (1)$$

2.1.2 Results and discussion Figures 5(a) and (b) show the average correlation coefficient grouping of each cutoff frequency. Figure 5(a) presents the results for the V-direction, while Fig. 5(b) presented the results for the H-direction. The average correlation coefficient in both directions decreases gradually with an increase in the cutoff frequency of the LPF. Further, the relative amounts of

reduction increase in both directions. For the maximum cutoff frequency (0.976 cycles/mm) in this verification, the average correlation coefficient in the V-direction decreases by 11% in comparison with the minimum cutoff frequency (0.039 cycles/mm). On the other hand, in the H-direction, a decrease of 3% in the average correlation coefficient was found. Moreover, an increase in each standard deviation was found with an increase in the cutoff frequency of the LPF in both directions. We attributed these results to a gradual increase in the interfusion of stochastic noise (white noise) when the cutoff frequency of the LPF was increased. Then, comparing the correlation coefficients of the V- (Fig. 5(a)) and H-directions (Fig. 5(b)), the correlation coefficient of the H-direction was relatively higher than that of the V-direction. Further, by increasing the cutoff frequency of the LPF, we found that the correlation coefficient of the V-direction decreased rapidly compared with the H-direction. As for the reasons for the different values and decreasing trends of the correlation coefficients in each direction, we considered that the stochastic noise had anisotropy, or that the V-direction was more susceptible to stochastic noise than the H-direction. However, the results of both directions showed very high correlation coefficient values. These results indicate that the same noise components could be extracted from each X-ray image despite their different radiographic factors. Therefore, we consider that our presumption and suggested extraction method, which use an LPF to extract stationary noise, may be valid.

Next, to extract stationary noise from an original image, using an X-ray dose of 20 mAs, we set the following two conditions with respect to the set up error and anisotropy of stochastic noise:

- I) The correlation coefficient was more than 0.98.
- II) The correlation coefficient did not decrease considerably.

The cutoff frequency of the LPF that fulfills the two conditions, which was determined to be 0.195 cycles/mm, was adopted for extracting stationary noise. Therefore, as shown in Fig. 6, we obtained a stationary noise image that was processed using an LPF (0.195 cycles/mm).



Fig. 6. The stationary noise image. An X-ray image processed using an LPF (cutoff frequency: 0.195 cycles/mm).

3. Identification of Stationary Noise Using Polynomial Regression Model

To perform a mathematical identification of stationary noise, we fit the mathematical model to the image shown in Fig. 6. As mentioned in Sec. 2, stationary noise may make it impossible to use a regular signal generation process in the signal distribution of X-ray images. This is because this process is intricately related with the unique characteristics of an X-ray imaging system, such as the nonuniformity distribution of the X-ray emission attributed to the imaging geometry, structural nonuniformity of the IP during the manufacturing process, and nonuniformity in the sensitivity of the IP readout system in the CR system. Therefore, as stationary noise consists of low-frequency components without spike-like noise, and stationary noise changes depending on its position within the X-ray image, we attempted mathematical identification using a polynomial regression model due to its flexibility.

3.1 Subjects and methods

To perform a specific identification, we used two verification methods. The first is a fitting method that uses a one-dimensional polynomial regression model utilizing the line profiles extracted from a stationary noise image. The second is a fitting method using a two-dimensional polynomial regression model that utilizes the stationary noise image directly.

First, in the line profile method, 1,024 line profiles were extracted in each of the two directions (V- and H-directions). Then, each line profile was fit in the one-dimensional polynomial regression model as described by Eq. (2):

$$E = z + a_1x + a_2x^2 + \dots + a_dx^d, \quad (2)$$

where E is the output value from the polynomial regression model, x is an independent variable, d is the maximum order of the polynomial regression model, and z and a_d are free parameters. In this case, d was set as 1 to 5. Further, each parameter was determined using the method of least squares. In order to evaluate the compatibility of each one-dimensional polynomial regression model, the determination coefficient was calculated from each line profile.

Next, in the method that directly utilizes the stationary

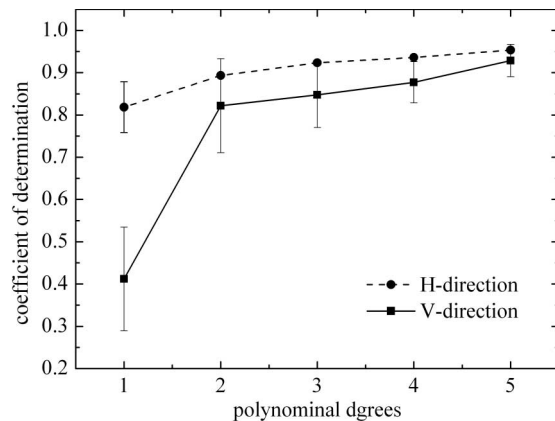


Fig. 7. Changes in the determination coefficient in the one-dimensional polynomial regression model.

noise image, the stationary noise images were fit in the two-dimensional polynomial regression model described in Eq. (3):

$$E = z + a_1x + a_2x^2 + \dots + a_dx^d + b_1y + b_2y^2 + \dots + b_dy^d, \quad (3)$$

where E is the output value from the polynomial regression model, variable numbers x and y are independent variables (for the V- and H-directions, respectively), d is the maximum order of the polynomial regression model, and z and a_d are free parameters. The order of model d was set to 1 to 5 as using the line profile method, and the orders of x and y were set as the same value. Each parameter was also determined using the method of least squares. To evaluate the compatibility of each two-dimensional polynomial regression model, we calculated the determination coefficient as using the line profile method. Moreover, each order of the model was evaluated using Akaike's information criterion (AIC) as described in Eq. (4) (Akaike, 1973, 1974):

$$AIC = N \ln \left(\frac{\sum_{i=1}^{1024} (E_i - \bar{E})^2}{N} \right) + 2K, \quad (4)$$

where E_i is a two-dimensional polynomial regression curve after determining each of the parameters, N is the number of monument points (1024×1024), and K is the number of free parameters.

3.2 Results

Figure 7 shows the results of applying the one-dimensional polynomial regression model to the line profiles extracted from a stationary noise image. The vertical axis of the graph displays the average value of the determination coefficient, while the horizontal axis is the polynomial degree. In the line profiles of the V-directions, we confirmed that the average determination coefficient of the first-degree polynomial model was much lower than for the other degrees. For the greater than second-degree polynomial models, the average value of the determination coefficient increased gradually with an increase in the degree of the polynomial model. The average value of the determination coefficient was 0.93 in the fifth-degree polynomial model. On the other hand, in the H-direction, the average value of the determination coefficient increased gradually

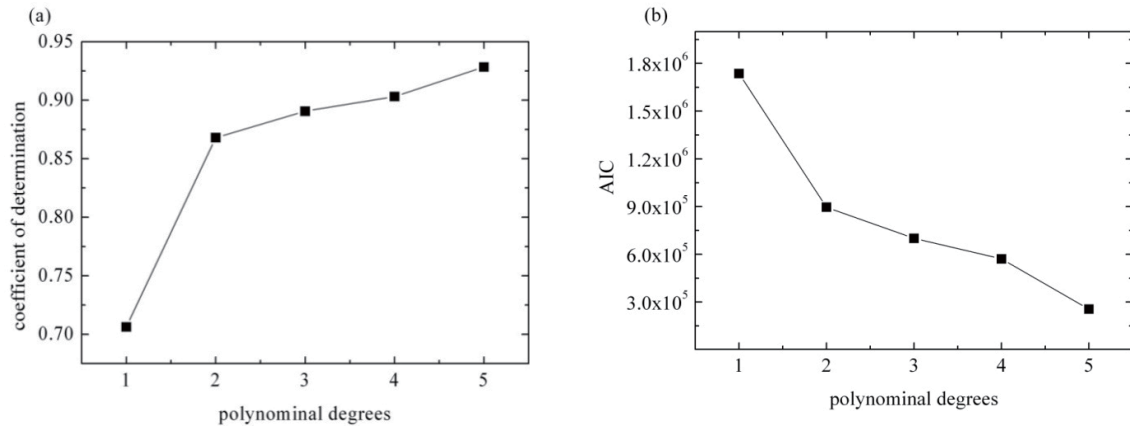


Fig. 8. Results of fitting the two-dimensional polynomial regression model directly to a stationary noise image: (a) determination coefficient and (b) AIC.

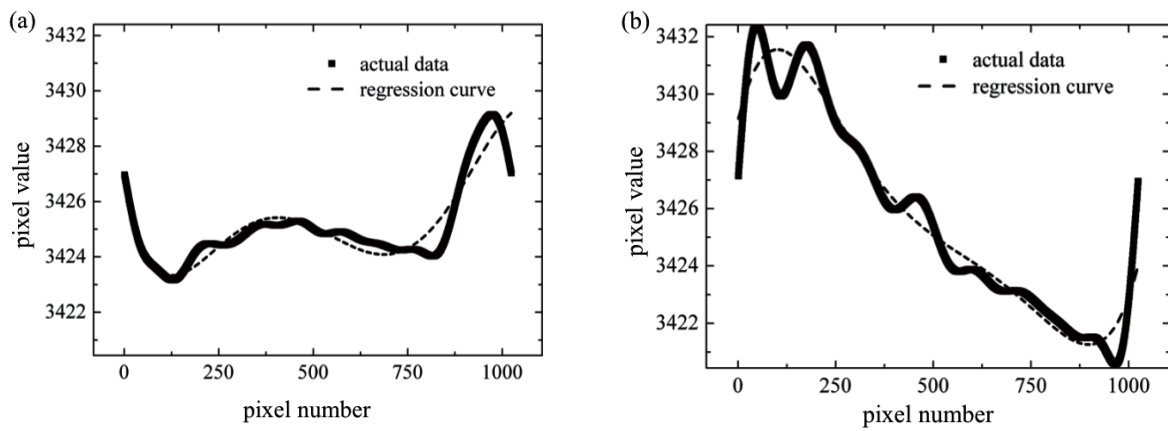


Fig. 9. Example of a line profile extracted from each direction, and a fifth-degree regression curve: (a) V- and (b) H-directions.

with an increase in the degree of the polynomial model, as demonstrated in the V-direction. The highest average value of the determination coefficient in the V-direction was 0.95 for the fifth-degree polynomial model.

Next, Figs. 8(a) and (b) show the results of applying the two-dimensional polynomial regression model to the stationary noise image directly. Figure 8(a) shows the results of the average determination coefficient. In the first-degree polynomial model, the average determination coefficient was much lower than in the greater than second-degree polynomial models. With an increase in the degree of the polynomial model, a gradual increase in the average value of the determination coefficient was found. The highest average value of the determination coefficient was 0.93 in the fifth-degree polynomial model in the H-direction. On the other hand, Fig. 8(b) shows the results of the AIC. The results of the AIC are opposite those of the determination coefficient. The AIC of the first-degree polynomial model was much higher than in higher-degree polynomial models. The AIC in the second-degree polynomial model decreased gradually with an increase in the degree of the polynomial model.

3.3 Discussion

In mathematical identification using the one-dimensional polynomial regression model, the determination coefficient

was calculated from 1,024 line profiles extracted from the stationary noise images in both the V- and H-directions. As a result, in the V-direction, the determination coefficient of the first-degree model was much lower than that of the other degree models. Moreover, the determination coefficient increased with an increase the in degree higher than the second-degree model (Fig. 7). We believe that these results were due to the configuration of the line profiles in the V-direction. The center line profile in the V-direction had a relatively low value, and the line profiles at both ends had relatively high values. Therefore, it is believed that applying the first-degree model did not duplicate the configuration of the line profile. On the other hand, in the case of the higher-degree models, the determination coefficient increased considerably due to gradually fitting the approximate configuration of the regression curve. To carry out regression, the polynomial regression model is generally able to be applied to a more difficult configuration by increasing the degree, which is due to an increase in the latitude of the regression curve. Therefore, in this study, it was also presumed that the determination coefficient increased gradually with an increase in the degree of the model. However, the polynomial regression model has a drawback of not passing all data points when performing regression at a low degree, compared with the amount of total data. More-

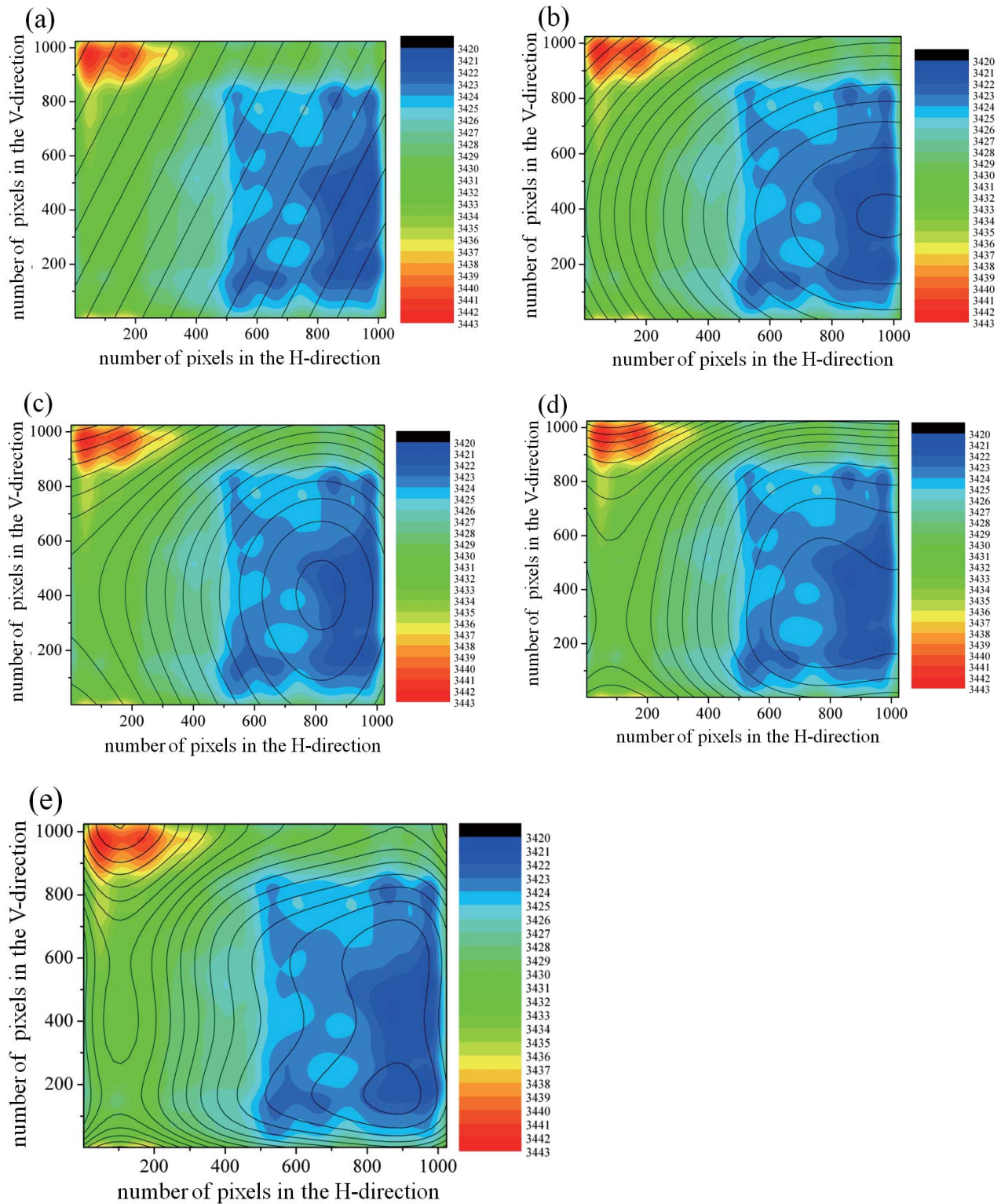


Fig. 10. Appearance when fitting different two-dimensional polynomial regression models of the (a) first-, (b) second-, (c) third-, (d) fourth-, and (e) fifth-degree.

over, the polynomial regression model also has a tendency to oscillate at both ends of the data. Figures 9(a) and (b) show examples of a line profile in each direction and a regression curve of the fifth-degree model. These line profiles were extracted from the center of a stationary noise image.

Each regression curve was able to capture the characteristics of the line profile almost exactly. However, for points with large variations in pixel value, or smaller fluctuations, the regression curve did not capture the line profile completely. Therefore, for capture flexibly, it was determined

that the model should be revised.

Next, in mathematical identification using the two-dimensional polynomial regression model, the determination coefficient and the AIC were calculated directly from the stationary noise images. As a result, the determination coefficient of the first-degree model was much lower than that of the other degree models. Moreover, the determination coefficient gradually increased when a greater than second-degree model was used. The results of the AIC indicated the opposite conclusion as the determination coefficient (Figs. 8(a) and (b)). For the first-degree model, it was conceivable that the determination coefficient was quite low, while the AIC was much higher, because the first-degree model did not apply a curved surface in the V-direction, as was the case when the one-dimensional polynomial regression model was fitted. Figure 10 shows the appearance when the two-dimensional polynomial regression model with the degree ranging from 1 to 5 is fitted. The colored map in Fig. 10 shows variations in pixel value, where the contour lines depict the appearance of a two-dimensional regression curve. From Fig. 10, we were able to find that the appearance of the contour line matched the distribution of the color map with an increase in the degree of the polynomial regression model. However, for the first-degree of the polynomial regression model, the contour line did not match the color map altogether. These results have excellent agreement with those of the determination coefficient and AIC. When the two-dimensional polynomial regression model is fitted, the reproduction ability of the complex configuration was lower than in the one-dimensional polynomial regression model because the pixel value at each position was determined by considering the characteristics of both directions. Therefore, the two-dimensional polynomial regression model fell short of duplicating the complex configuration completely. Further, we also considered that it was very difficult to completely duplicate the complex configuration if regression was carried out using higher than a fifth-degree polynomial regression model.

In light of these results, it was possible that the stationary noise was able to be partially acquired by applying a higher than second-degree polynomial regression model. Further, it was considered that the stationary noise was duplicated with more precision when increasing the degree of the polynomial regression model. However, the results of regression by both the one-dimensional and two-dimensional models show that increasing the degree of the polynomial regression model did not achieve significant improvement in the determination coefficient or AIC. Moreover, it remains possible that the amount of improvement achieved when fitting the model was low as compared to the increase in the amount of calculation attributed to an increase in the model degree. Therefore, for an accurate mathematical identification of stationary noise, we suggest modifying the polynomial regression based model, for instance, by capturing a more difficult variance, rather than increasing the degree of the polynomial regression model.

4. Conclusions

In this paper, we verified a method for extracting stationary noise. Further, we also performed mathematical identification of stationary noise using a polynomial regression model as a fundamental study of the development of a noise rejection method using a mathematical model that realizes an accurate digital X-ray imaging system.

The results show that stationary noise can be extracted with high precision using a particular LPF frequency. Next, we performed mathematical identification of stationary noise using a polynomial regression model. As a result, we found that a greater than second-degree polynomial regression model can roughly identify stationary noise. Moreover, it became possible to identify stationary noise in more detail by increasing the degree of the model. However, the fitting accuracy of the regression curve was not significantly improved in terms of the amount of calculation required to increase the degree of the polynomial used in the regression model. Therefore, we believe that retrieval should be added to a basic polynomial regression model to accommodate variations of stationary noise with increased flexibility.

In this paper, the identification of the stationary noise was verified using a single X-ray image. Thus, in the future we will attempt to build a mathematical model that realizes accurate characteristics of stationary noise using retrieval and identification based on multiple X-ray images. Moreover, stochastic noise will also be verified. Eventually, we expect that this study will contribute toward an improvement in diagnostic imaging through identification of the form of an image noise and the development of a correct mathematical model.

References

- Akaike, H. (1973) Information theory and an extension of the maximum likelihood principle, in *Second International Symposium on Information Theory* (eds. N. B. Petrov and F. B. Csaki), pp. 267–281, Akadémiai Kiadó, Budapest.
- Akaike, H. (1974) A new look at the statistical model identification, *IEEE Trans. Automatic Control*, **19**, 716–723.
- Barnes, G. T. (1982) Radiographic mottle: A comprehensive theory, *Med. Phys.*, **9**, 656–667.
- Dobbins, J. T., III, Samei, E., Ranger, N. T. and Chen, Y. (2006) Intercomparison of methods for image quality characterization. II. Noise power spectrum, *Med. Phys.*, **33**, 1466–1475.
- Kono, M. and Adachi, S. (2008) The role of plain chest radiograph in lung cancer diagnosis, *Japanese Journal of Lung Cancer*, **48**(1), 11–19.
- Kunitomo, H., Ichikawa, K., Higashide, R., Ohashi, K. and Sawada, M. (2010) Investigation of error factors in analysis of digital noise power spectrum, *Jpn. J. Radiol. Technol.*, **66**(7), 734–742.
- Ogawa, E., Arakawa, S., Ishida, M. and Kato, H. (1995) Quantitative analysis of imaging performance for computed radiography systems, in *Proc. of SPIE Medical Imaging*, 2432, pp. 421–431.
- Rossmann, K. (1963) Spatial fluctuations of X-ray quanta and the recording of radiographic mottle, *Am. J. Roentgenol.*, **90**, 863–869.
- Yamada, S. and Murase, K. (2005) Effectiveness of flexible noise control image processing for digital portal images using computed radiography, *Br. J. Radiol.*, **78**, 519–527.